COMPACT MULTI-PURPOSE OPTICS INSERTION IN THE FERMI@ELETTRA LINAC BUNCH COMPRESSOR AREA

S. Di Mitri#, M. Cornacchia, Sincrotrone Trieste (ELETTRA), Trieste, Italy

Abstract

The optics design of the first bunch compressor area in the FERMI@elettra linac is presented. Several constraints on the Twiss parameters are set by the preservation of beam quality in the first magnetic compressor, the optimization of diagnostics performance, the collimation process and the beam matching to the downstream lattice. A compact multi-purpose arrangement of magnetic and diagnostic elements is presented that, in principle, satisfies several different needs over a total length of 14m.

MOTIVATIONS

We report on the optics design of the FERMI@elettra [1] first compressor (BC1) area shown in Figure 1, relying on the analytical basis presented in [2–4] but completely renovated since 2008 in terms of compactness, magnetic and diagnostic layout. Changes are motivated by the adoption of a sole optics for beam diagnostic and transport purpose and to save space for acceleration. The multi-purpose optics insertion has been placed after BC1 because of several reasons: i) the beam can be characterised as function of the compression factor; ii) emittance ε_x and energy spread $\sigma_{\delta,CSR}$ blow up due to Coherent Synchrotron Radiation (CSR) [5] can be detected without additional spurious effects, i.e. those from structural wakefields [6,7]; iii) the low ~250MeV BC1 energy allows a higher measurement resolution of the particle energy distribution than at the linac end; iv) an insertion for optics matching and a first stage of geometric collimation had to be placed after BC1 anyway, forcing to dedicate some space for no acceleration items.

OPTICS CONSTRAINTS AND SOLUTION

The constraints on the Twiss parameters in the BC1 area are listed below, in the order of priority, with reference to Figure 1.

1) The horizontal betatron function β_x has to be shrunk to the 1m level to minimize the CSR induced emittance growth [5], i.e. according to $\Delta\varepsilon_x/\varepsilon_x \approx 0.5\beta_x\theta^2\sigma_{\delta,CSR}$.

2) The effective strength of the vertical RF deflector (LERFD) $\propto$ $S_y=(\beta_{1,y}\beta_{2,y})^{1/2}\sin\Delta\mu_{x,y}$ (containing 3 independent optics parameters), the transport matrix element from LERFD to one of the screens in the straight line and the one in the dispersive line. It must therefore be maximized by a suitable optics.

3) The choice of a sole optics for diagnostic and transport purpose suggests to adopt a periodic phase advance $\Delta\mu_{x,y}$ pattern, so that the $\varepsilon_{x,y}$ measurement can be done with the multi-screen technique, alternative to the usual quadrupole scan.

4) A small β_x and a high horizontal dispersion η_x are required at the screen in the spectrometer line to characterize the particle energy distribution.

5) The 4 independent Twiss parameters $\alpha_{x,y}$ and $\beta_{x,y}$ have to be matched somewhere in the area to keep the optics under control (i.e., sufficiently smooth) and to match the beam to the downstream linac lattice.

6) A proper setting of high $\beta_{x,y}$ and $\Delta\mu_{x,y}\cong\pi/2$ has to be set in the area to allow geometric collimation.

All quadrupoles involved have bipolar power supply for a larger acceptance in case of largely mismatched beam from the injector. Four quadrupoles along the upstream Linac1 (see Figure 2) are used for point 1. They naturally excite a high β_y=68m at the end of BC1, where we have put LERFD (point 2). Downstream of BC1, 5 quadrupoles over 2.5m with an average integrated strength of k_1l=0.18m^{-1} build a low-β symmetric optics, as shown in Figure 2, with $\Delta\mu_{x,y}=2\pi/3$ over the following 10m (points 3 and 5). The beam waist is at the central screen where $\beta_{x,y}$ =3m. Collimators are near each of the outer two screens (point 6), although $\beta_{x,y}$ =12m there is not as big as wished. Due to the optics symmetry, the collimators are identical (saving costs), with cylindrical apertures to collimate both planes at the same location and sufficiently long to guarantee a full absorption [8], so avoiding the usual spoiler plus absorber scheme. Since the distance between the screens $\propto$ $\beta_{x,y}$ at the collimators, the total length of the insertion is a compromise between available space and collimation efficiency.

Not to add space in the z-direction, a dipole magnet (spectrometer) has been inserted between the last two screens. It deflects the beam horizontally in the dispersive line to measure the energy distribution. A FODO cell has been added upstream of the dipole (this is switched off during the machine operation), downstream of it in the dispersive line and in the straight line. The first two cells balance the geometric and the chromatic contribution to the particle motion (point 4), so improving the measurement resolution. The third cell completes the matching to the downstream linac.

The whole multi-purpose insertion in the BC1 area is 14m long. Space has been saved by using the upstream linac focusing to match the optics both in BC1 and in LERFD. Only one additional matching station after LERFD is sufficient to satisfy all other constraints.

The optics also allows a suitable trajectory correction scheme made of 4 Beam Position Monitors (BPMs) and 6 corrector magnets (CHV) per plane (combined devices). Redundancy is present near the dipole. The scheme allows one to measure the residual dispersion out of BC1, to build a straight line along the 5 matching quadrupoles, to measure the residual field of the dipole and to launch the beam into the succeeding linac.

#simone.dimitri@elettra.trieste.it

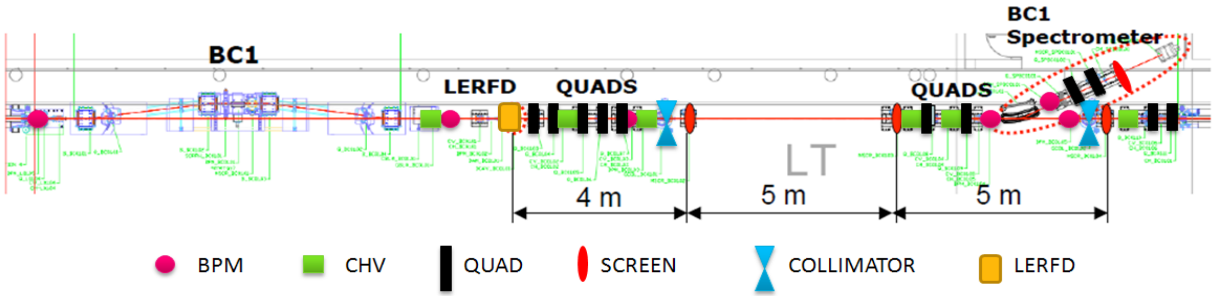

Figure 1: Schematic layout of the BC1 area.

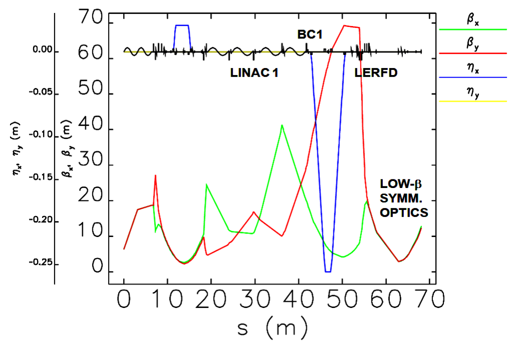

Figure 2: Optics from the Gun to the BC1 area.

STRAIGHT LINE

Projected $\varepsilon_{x,y}$ can be measured by scanning the strength of the last matching quadrupole and looking to the beam size at the second screen, or with the 3-screens technique without changing the nominal optics.

The bunch is vertically deflected according to the product of the RF kick from LERFD and the effective length S_y [3]. This is 5m, 14m and 22m from the 1^{st} to 3^{rd} screen, respectively. The last one should therefore be used for bunch length measurement. Linear transport analysis translates there a 1ps full width long bunch into a 6.7mm vertical spot size. Since the non-deflected rms beam size is 0.1mm, 6.7/4·0.1=15 longitudinal slices could be resolved in principle. A conservative picture of 10 slices ~ 100fs resolution could be considered to reduce the bunch length measurement error down to 1% [3] or just in case of shorter bunches.

The slice horizontal emittance is foreseen to be measured with quadrupole scan at the 2^{nd} screen, taking advantage of the natural beam waist. The expected minimum horizontal beam size is 60µm, so that a 10µm rms screen+CCD resolution has been specified. The quadratic behavior of σ_x^2 vs. quadrupole strength can be analytically predicted. During the scan, a bunch length in the range 0.5-1.5ps is expected to be translated into a vertical spot size in the range 4-8mm. The optics has been designed to resolve here 100fs at 330MeV.

DISPERSIVE LINE

The ratio $\eta_x/\sqrt{\beta_x}$ determines the optical resolution of the beam energy measurement [9]. It is $0.09\text{m}^{1/2}$ at the BPM and $0.8\text{m}^{1/2}$ at the screen. The BPM has been thought to be used to find the accelerating crest of the upstream linac over a wide range of RF phases by looking to the bunch centroid position. The absolute energy measurement at the screen is limited by the still high Δ_{SC}=20µm rms screen+CCD resolution to $\Delta_{SC}/\eta_x=4\cdot10^{-5}$, i.e. 12keV rms at 300MeV. The expected 0.1% mean energy jitter [10] can also be clearly detected both at the screen and at the BPM. The total energy spread $\sigma_{\delta,tot}$ will be in the range 0.5-2% for <E>=200–300MeV, depending on the compression scheme. The relative measurement error is limited [9] to $\delta_{res}=\sqrt{\varepsilon_x}/\sqrt{\beta_x}\cdot\sin(\theta/2)=3\cdot10^{-4}$, i.e. $\sigma_{\delta,tot}$=1–6MeV ±340keV.

With LERFD, the longitudinal phase space can be reconstructed at the screen. The target size accommodates a 2% energy spread, 10ps long bunch. The $\sigma_{\delta,slice}$ measurement resolution is limited by Δ_{SC} to 8–12keV rms at 200–300MeV. At the same time, $\sigma_{\delta,slice}$ not smaller than $1\cdot10^{-4}$ should be measured to avoid in turn a big error (>10%) due to the contribution of the geometric optics:

$$\frac{\sigma_x(\delta)-\sigma_{x,0}}{\sigma_{x,0}}=\sqrt{1+\kappa^2}-1 \qquad (1)$$

where $\kappa=(\varepsilon_x\beta_x)^{1/2}/\eta_x\sigma_\delta$. Δ_{SC} always dominates the resolution. Assuming the central value at least ~3 times larger than the error, then the best analytical estimation is $\delta_{rms,slice}$=30keV±12keV at 300MeV.

GEOMETRIC COLLIMATION

A collimation system (CS) is primarily required to avoid that halo particles hit the undulator vacuum chamber, whose vertical half-aperture is 3.5mm, so creating showers that could induce demagnetization of the permanent magnets. A 1-D analytical expression for the geometric collimation efficiency that is independent from the particle distribution has been derived in [4], as function of $\beta_{x,y}$ and $\Delta\mu_{x,y}$. A collimator half-aperture of 2mm for $\Delta\mu_{x,y}=2\pi/3$ completely shadows the undulator chamber. However, to make the CS more flexible in terms of beam acceptance, two other optional half-apertures of 3 and 4mm radius have been inserted in the same device. Nominally these apertures do not shadow the undulator chamber but are still able to stop particles traveling at amplitudes larger than the mentioned gap. The real efficiency and stopping power of the CS should then be verified by tracking more detailed halo particle distributions and, of course, verified in commissioning.

ERRORS ESTIMATION

The measurement errors in the dispersive line have already been discussed. A first estimate of the order of magnitude of the error affecting the projected ε measurement can be done by assuming an exact value for β and 10μm screen resolution, Δσ, to detect a full width spot size of 5 standard deviations, 5σ, where the smallest expected beam size is σ=60μm. Thus, $\Delta\varepsilon/\varepsilon=2\Delta\sigma/\sigma\cong 6\%$. This error can be reduced by a fitting procedure with many measured points. Since the horizontal and the vertical dynamics are uncoupled, the same considerations apply to the projected and slice ε (once the slice length is correctly detected).

The minimum detectable slice length has previously been discussed. Nevertheless, a careful design of the quadrupole focusing downstream of LERFD has to be carried out because, in the case of a fully compressed and deflected beam, the magnets are traversed by a 2% rms energy spread, vertically large sized beam. The chromatic aberration induced by the quadrupole field can be evaluated in the pessimistic scenario of complete filamentation as follows:

$$\Delta x, \Delta y \le \frac{1}{|k_1 l|\sigma_\delta}\sqrt{\frac{2\varepsilon_y}{\beta y}\frac{\Delta\varepsilon_y}{\varepsilon_y}} \qquad (2)$$

where Δx, Δy is the beam distance from the quadrupole magnetic axis. For practical purposes, (1) is an indication of the chromatic optics distortion. For a non-deflected beam, we expect $\Delta x,\Delta y \le 300\mu m$ where $k_1 l \le 0.26 m^{-1}$ and $\beta \le 68m$, so giving $\Delta\varepsilon/\varepsilon \le 5\%$. The strongest quadrupole is the closest to LERFD, so that for a deflected beam the particle vertical displacement couples in a relevant way to the quadrupole filed only in the last two weaker magnets of five. For a 1ps long bunch, we have in these quadrupoles $\Delta y \le 500\mu m$ (this really applies only to the deflected bunch edges), $k_1 l \le 0.14 m^{-1}$ and $\beta \le 68m$, so giving again $\Delta\varepsilon/\varepsilon \le 5\%$.

The dipole kick of the quadrupoles traversed off-axis affects not only the motion of the bunch centroid (trajectory distortion) but also the linear dependence of the deflecting kick with the longitudinal position inside the bunch [3]. In other words, the path of particles distant from the quadrupole axis will be distorted by the quadrupole field, finally corrupting the effective magnification factor of the deflecting process at the screen. It is straightforward to evaluate that the maximum quadrupolole kick $k_1 l \cdot \Delta y \cong 50\mu rad$ is much smaller than the LERFD kick $zV_{RF}\omega_{RF}/Ec$ for z=500μm, corresponding to 1mrad. Particle cross-over between adjacent slices is therefore excluded.

As a preliminary check of the linear analysis used so far, *elegant* code [11] has been applied to a 330pC, 1ps long bunch after not linearized magnetic compression, as shown in Figure 3. The 6.5mm bunch length at the 3rd screen shown in Figure 3 and the slice ε_x measurement at the 2nd screen shown in Figure 4 are in full agreement with the analytical predictions discussed in the previous Sections. The whole current spike is contained in the first 0.65mm long slice at the screen.

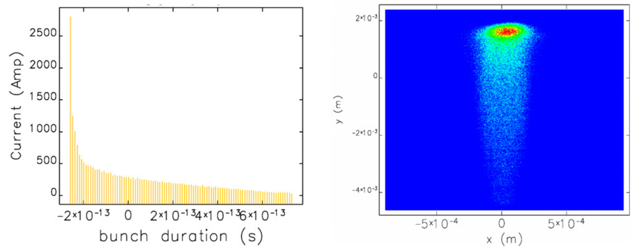

Figure 3: Current profile (left) and deflected beam at the 3rd screen (right).

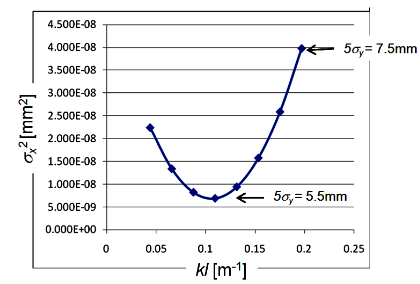

Figure 4: σ_x^2 vs. quadrupole strength at the 2nd screen.

COMMENTS

The validity of this linear optics analysis could be limited by a non-uniform charge distribution affecting the equal-spatially slice division of the bunch length assumed so far. The 100fs resolution of the LERFD is still far from the cooperation length of the free electron laser process at few nm wavelengths. The positioning of quadrupoles downstream of LERFD also makes the measurements sensitive to optics matching and trajectory control. Finally, high collimation efficiency is provided only by the smallest 2mm aperture, less manageable from the beam transport point of view. A dedicated optics for collimation with bigger $\beta_{x,y}$ would have been desired. However, a different set-up, i.e. quadrupoles upstream of LERFD, would require more space downstream of it to reach a waist or, equivalently, a smaller $\Delta\mu_{x,y}$, in conflict with the needs of the CS that should be moved further downstream in a dedicated location with additional focusing. Further modifications to the present magnetic lattice are still possible but probably not in the picture of a sole optics for beam diagnostic and transport.

REFERENCES

[1] C.J. Bocchetta et al., FERMI@elettra CDR (2007).
[2] P. Craievich et al., EPAC'08, Genoa, I (TUPC080).
[3] P. Craievich et al., Fermi Note ST/F-TN-07/09 (2007).
[4] S. Di Mitri, PRST-AB **13**, 052801 (2010).
[5] Y. Derbenev et al., TESLA-FEL 95-05 (1995).
[6] M. Cornacchia et al., PRST-AB **9**, 120701 (2006).
[7] P. Craievich et al., NIM A **604** (2009) 457–465.
[8] S. Ferry et al., Proc. of PAC'09, Vancouver, Canada.
[9] see for example, H. Wiedemann, Particle Accelerator Physics – Vol.I, edited by Springer (1998).
[10] P. Craievich et al., EPAC'06, Edinburgh, Scotland, UK (THPCH043).
[11] M. Borland, APS LS-287 (2000).